JOURNAL OF MATERIALS SCIENCE 21 (1986) 2590–2596

Passivity, pitting and corrosion of anodically polarized Fe–Ni alloys in 0.5 M H_2SO_4 containing Cl^-

W. J. TOMLINSON, S. A. CAMPBELL*
Department of Applied Physical Sciences, Coventry (Lanchester) Polytechnic, Coventry, UK

Iron–nickel alloys containing 0, 20, 40, 60, 80 and 100% Ni (wt%) have been anodically polarized in 0.5 M H_2SO_4 containing Cl^-, and the conditions for passivity, pitting and corrosion with respect to alloy composition and Cl^- concentration broadly defined. Breaks occur in the values of the corrosion properties at about 30% and 70% Ni. It is considered that the corrosion properties of alloys containing up to 30% Ni are determined by the ferrite in the alloy and the low corrosion resistance of its surface film, that alloys containing 30 to 70% Ni have a corrosion resistant film probably similar to a nickel ferrite spinel, and that alloys containing over 70% Ni have properties similar to nickel and probably have a surface film based on a solid solution of iron in NiO.

1. Introduction

Alloys, rather than pure metals, are mostly used in service and considerable effort is directed towards characterizing their corrosion behaviour, particularly with respect to the presence of chloride ions, which frequently initiates local attack. Both iron and nickel are of great industrial importance and corrosion studies on the Fe–Ni system have attempted to relate changes in the corrosion behaviour to changes in the alloy composition, with particular interest in the composition of the alloy which separates the alloys with iron-like behaviour from those with nickel-like behaviour. Using various corrosion parameters changes have been observed at 50% and 30% Ni [1], between 40 and 60% Ni [2], 40% Ni [3], and between 51 and 70% Ni [4]. (All percentages, unless given otherwise, are in weight per cent.) No obvious relation to the crystal structure appears to exist in these and other [5, 6] data, and the use of the Uhlig electronic configuration theory [7], which predicts nickel-like behaviour in alloys containing more than 34% Ni, appears to be indecisive [3]. Intergranular corrosion has been observed in an Fe–31% Ni alloy [8] and localized attack may occur in the presence of chloride ions. Corrosion of an Fe–25% Ni alloy [9, 10] and of an Fe–36% Ni alloy [11] has been observed to be greatly affected by the presence of chloride ions and pitting, an increase in the passivation current, and eventually continuous dissolution, occurred as the concentration of chloride was increased [9–11].

Corrosion studies on a series of alloys have the additional advantage of showing the influence of the alloying elements on the corrosion processes, and the present work aims to eastablish the general pattern of passivity, pitting, and corrosion of iron-nickel alloys across the composition range, in 0.5 M H_2SO_4 containing various amounts of chloride ions.

2. Experimental procedure

The composition of the alloys are shown in Table I. The iron and 20% Ni alloy were supplied by the British Steel Corporation, UK, and contained the following analysed residual impurities (wt%): Ni 0.003 (for pure iron), C 0.0014,, N 0.0017, Si 0.01, S 0.005, P 0.002, Cr 0.02, Cu 0.011, Al 0.01. The higher nickel alloys were supplied by Inco Alloys International Ltd (Birmingham, UK) and the analysed residual impurities were less than (wt%): C 0.005, Cr 0.05, Co 0.1, Mo 0.01, Ti 0.05, Al 0.1, Si 0.2, Mn 0.05, Zn 0.01, Cu 0.05. All the alloys were vacuum melted, forged, rolled, machined, annealed in H_2 at 1300° C for 2 h, and then furnace cooled. Metallographic examination showed all the alloys to have an apparently single phase microstructure. Alloys containing 40 to 100% Ni consisted of large equiaxed grains containing annealing twins while the pure iron and the 20% Ni alloy consisted of more irregular outlined smaller grains. All the alloys were metallurgically very clean except the 20% Ni alloy which contained a relatively large number of non-metallic inclusions. X-ray diffraction (XRD) showed the iron and 20% Ni alloy to be b c c and the higher nickel alloys to be f c c. In particular, there was no evidence of super-lattice lines in the 80% Ni alloy. The Fe–Ni alloys after annealing have been shown to be b c c up to 25% Ni [6] and $\alpha + \gamma$ from 10 to 40% Ni [2]. In view of these differences the crystal structure of the 20% Ni alloy was checked by XRD to be b c c and the composition analysed by X-ray fluorimetry (XRF) to be 19.5% Ni. This is close to the value of 19.34% Ni in Table I determined by the suppliers. Distilled water and Analar reagents were used to make the solutions.

Specimens of known cross-section and approximately 20 mm^2 were set in a polytetrafluoroethylene PTFE holder with epoxy resin, polished to a 600 grit

---

Present address: Department of Chemistry, Southampton University, Southampton, UK.

0022–2461/86 $03.00 + .12

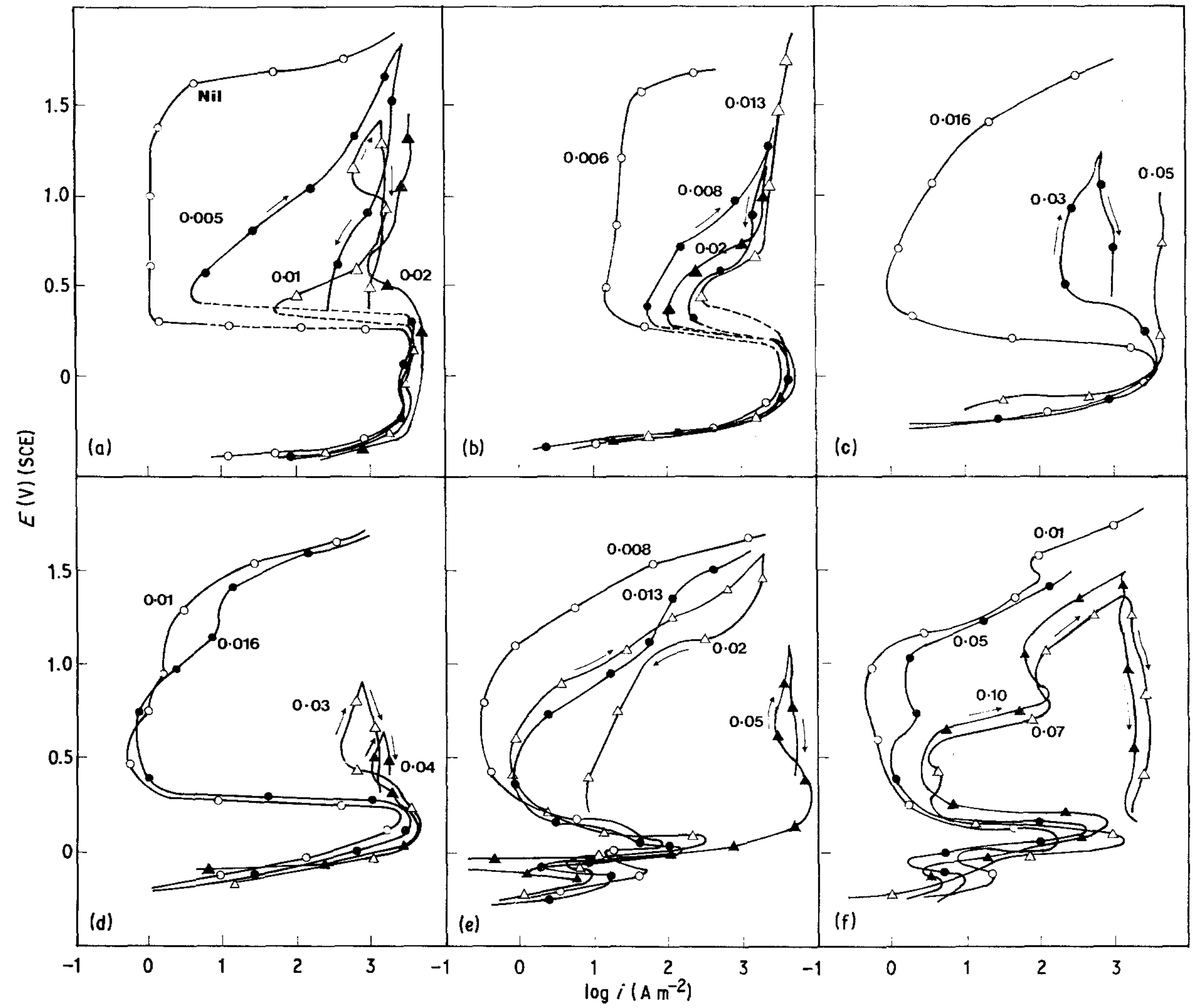

Figure 1 Anodic polarization behaviour of representative Fe–Ni alloys in deoxygenated 0.5 M H_2SO_4 containing Cl^-. The curve numbers refer to the concentration of Cl^- in mol dm^{-3}. (a) iron; (b) 20% Ni; (c) 40% Ni; (d) 60% Ni; (e) 80% Ni; (f) nickel.

finish and degreased in ethanol. A standardized potentiodynamic polarization procedure was used. Nitrogen was bubbled through the solution for 30 min and throughout the test. The rest potential was taken after 10 min, and then the specimen was cathodically cleaned at -1.5 V (SCE) for 10 min before anodically ramping at 1 mV sec^{-1} from -1.3 V (SCE). If the surface was passive the run was terminated when oxygen was evolved. If pitting was observed the ramp was reversed when the current density reached approximately 10^3 A m^{-2} and was continued until the current began to rise again near the active peak. On completion of the run the specimen was washed and dried. A limited survey of pit morphology was undertaken using optical microscopy.

3. Results and discussion

Some results of the anodic polarization behaviour of iron–nickel alloys in 0.5 M H_2SO_4 containing different amounts of Cl^- are shown in Fig. 1, and various derived corrosion parameters from all the results are presented in Table II. For clarity some results are omitted from Fig. 1, but in all cases the omitted results follow the pattern of behaviour. This is shown by the corrosion parameters from the collected data in Table II and Figs 2–4. The focus of the present work is the pattern of anodic characteristics of the Fe–Ni alloy series in 0.5 M H_2SO_4/Cl^-, and the pure iron and pure nickel end-members are considered only briefly with respect to the large body of literature on these metals.

TABLE I Alloy compositions

	wt % : 0 (pure Fe)				
Actual nickel	19.34	40.5	59.9	79.9	100
Nominal nickel	20	40	60	80	100

The free corrosion potential (E_{corr}) is shown in Fig. 2 as a function of the alloy composition and chloride concentration of the solution, The values of -477 and -265 mV for pure iron and pure nickel, respectively, in chloride-free solutions compare favourably with the values -470 to -517 mV and -262 and -323 for iron and nickel, respectively, obtained by previous workers [2, 3, 5, 10]. Chloride ions have only a small effect on E_{corr} (Fig. 2); this is consistent with results obtained on nickel [12] and on an Fe–25% Ni alloy [10]. While the open circuit potentials of a metal are a useful means of indicating the reproducibility of surface preparation, their diagnostic value is limited unless the formation and breakdown of the surface compounds are studied [13]. However, the trend in E_{corr} with alloy composition is clear (Fig. 2). Austenitic alloys (40 to 100% Ni) behave similarly to the electrochemically less active nickel. The 20% Ni alloy has an α structure and it is

TABLE II Corrosion parameters of the anodic polarization of Fe–Ni alloys in deoxygenated 0.5 M H_2SO_4 containing Cl^-

Alloy	$[Cl^-]$ (mol dm^{-3})	E_{corr}(SCE) (mV)	E_{pass}(SCE) (mV)	$i_{p,min}$ (A m^{-2})	i_{max} (A m^{-2})
Pure iron	nil	−477	320	0.33	3700
	0.005	−482	440	3.85	3400
	0.01	−490	450	44	3450
	0.02	−500	–	825	4500
	0.05	−493	–	3400	4100
	0.10	−437	–	≈5000	≈5000
20% Ni	0.004	−403	350	11.7	4050
	0.006	−380	420	14.3	3390
	0.008	−410	–	52.9	4000
	0.013	−390	–	201	4370
	0.020	−397	–	103	4600
40% Ni	0.016	−295	530	0.91	3620
	0.030	−293	–	200	4050
	0.050	−282	–	3610	4600
50% Ni	0.005	−300	150	0.14	3270
	0.010	−300	500	0.41	3490
	0.025	−270	500	28.6	4670
	0.05	−288	–	2720	4350
	0.07	−282	–	4800	5000
60% Ni	0.010	−250	500	0.44	2640
	0.016	−250	480	0.75	3380
	0.03	−267	–	377	4130
	0.04	−240	–	992	3930
80% Ni	0.008	−275	550	0.30	75.7
	0.013	−250	450	0.81	158
	0.02	−245	450	0.74	307
	0.05	−240	–	2650	7800
Pure nickel	nil	−265	350	0.15	26.5
	0.01	−295	500	0.46	159
	0.05	−338	400	0.97	385
	0.07	−315	250	3.11	1240
	0.10	−330	400	2.65	796

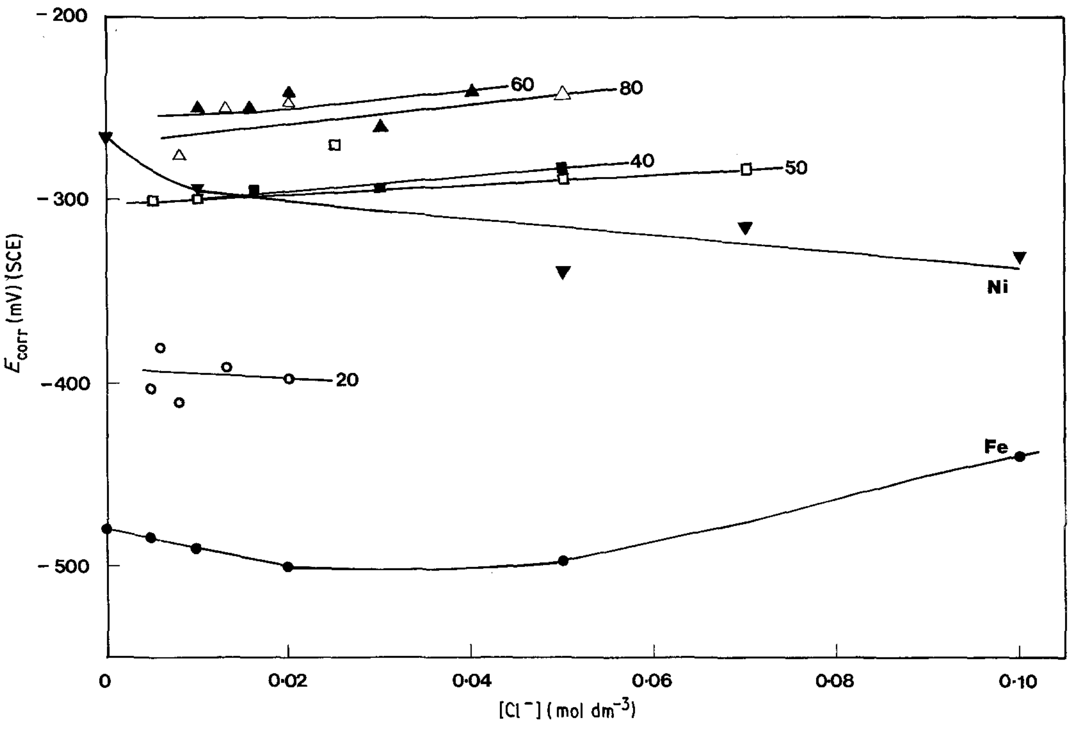

Figure 2 Corrosion potential of Fe–Ni alloys in 0.5 M H_2SO_4 containing Cl^- (Curve labels refer to wt % Ni.)

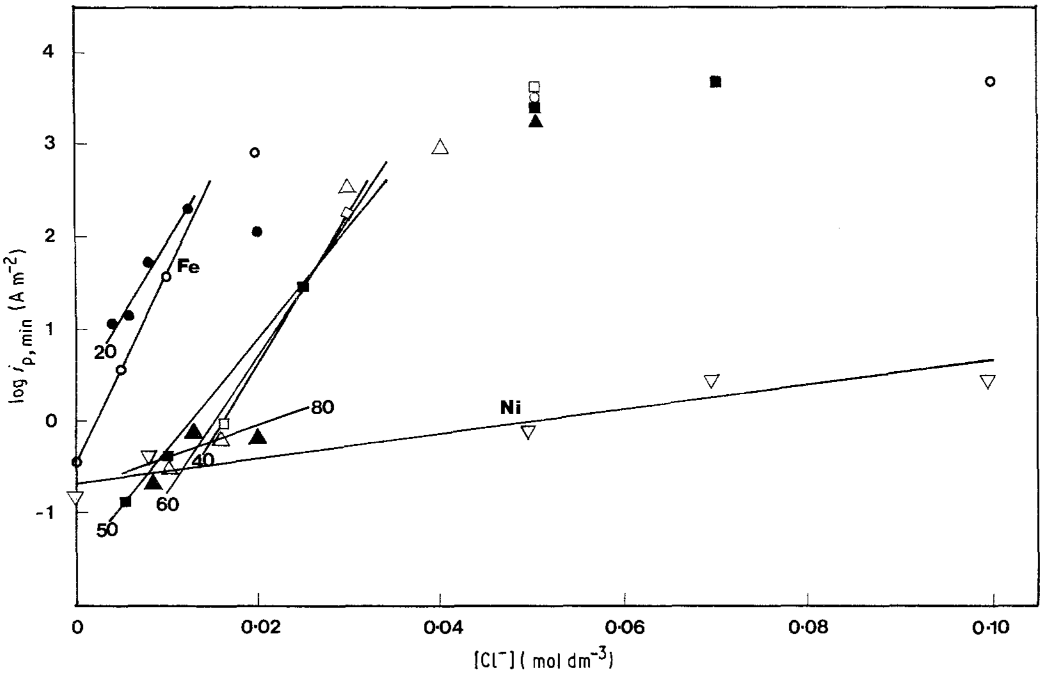

Figure 3 The minimum passivating current density as a function of [Cl$^-$] of Fe–Ni alloys anodically polarized in 0.5 M H_2SO_4.

clear the raised E_{corr} reflects the high concentration of nickel dissolved in the ferrite. The reasons why E_{corr} for nickel decreases with increase in Cl$^-$ while for alloys it increases with increase in Cl$^-$ are not clear. It may be associated with the properties of nickel–chloro complexes assumed to exist [12], or with the higher catalytic activity of an Fe–Ni surface compared with that of the pure metals [14]. These same factors may also be responsible for the raised value of E_{corr} for the 60 and 80% Ni alloys (Fig. 2) instead of the monotonically increasing values previously found in chloride-free solutions [2, 3, 5, 6]. This point is considered further below.

Alloys containing up to and including 60% Ni have similar large active loops, are little affected by Cl$^-$, and have an i_{max} of about 3000 to 4000 A m^{-2}. In contrast, the 80% Ni alloy and pure nickel have similar but much smaller active loops with a double peak, are affected by Cl$^-$, and have a much lower i_{max} (Fig. 1 and Table II). The double passivation peak observed in pure nickel, and also in the 80% Ni alloy (Fig. 1), is due to the formation of [$Ni(OH)_2 \cdot NiOOH$] and its subsequent electro-oxidation to NiO at higher potentials [15]. Chloride is stated to be specifically adsorbed on a metal surface [16–18] and this would lower the potential of the inner Helmholtz plane and so alter the dissolution rate. However, it had been observed that the active loop is relatively unaffected by the presence of Cl$^-$ with pure iron [19] and an Fe–25% Ni alloy [10], and these are in agreement with the present results on alloys containing up to 60% Ni. The manner by which the iron–chloro complexes leave the dissolution processes relatively unaffected, while the nickel–chloro complexes progressively increase i_{max} as the Cl$^-$ is increased, is not known. The present results on active dissolution indicate that the active anodic behaviour is controlled by iron in alloys containing up to 60% Ni and by nickel in alloys containing 80% Ni and above. Other workers have considered iron-like behaviour to extend to 50% Ni [6], and nickel-like behaviour above 70% Ni [4].

As the concentration of Cl$^-$ increases the current density in the passive state (i_p) increases, and the minimum current density in the passive state as a function of Cl$^-$ concentration is shown in Fig. 3. It is emphasized that the plot is for convenience in comparing the data and does not necessarily imply a log-linear function. The scatter is large, and the highest current densities clearly relate to continuous dissolution. Using the lower current densities, and their extrapolated values, the alloys appear to fall into three groups. For alloys containing up to 60% Ni the rates (of i_p with respect to [Cl$^-$]) are high compared to those of the 80% Ni and pure nickel. Within the alloys with a high rate there is a division based on the value of i_p (measured or extrapolated) when the concentration of Cl$^-$ is zero; the austenitic alloys (40 to 60% Ni) have a much lower value of i_p than the ferritic alloys.

Clearly the three groups reflect the type and nature of the passivating film on the different alloys and the influence of Cl$^-$ on the film structure and properties. A recent analysis of passive films on individual α and γ grains of an austeno-ferritic stainless steel using microscopic ellipsometry [20] have established that the passive films on γ-grains are thinner but more corrosion resistant than those on α-grains. This is consistent with the present grouping of alloys containing up to 60% Ni into those with an austenitic structure (40 to 60% Ni) and a low i_p, and into those with a ferritic structure (up to 20% Ni) and a high i_p (Fig. 3).

The nature of the structure and nonstoichiometry of passivating layers is complex and unresolved [21]. Some of the many structures formed on pure iron have recently been reviewed [22], but for simplicity we may consider the film as a complex oxide, perhaps polymeric [21, 23], approximating to Fe_3O_4 and Fe_2O_3 at its inner and outer surfaces with the whole being stabilized by an adsorbed layer of oxygen molecules [24, 25]. Surface films on nickel consist essentially of

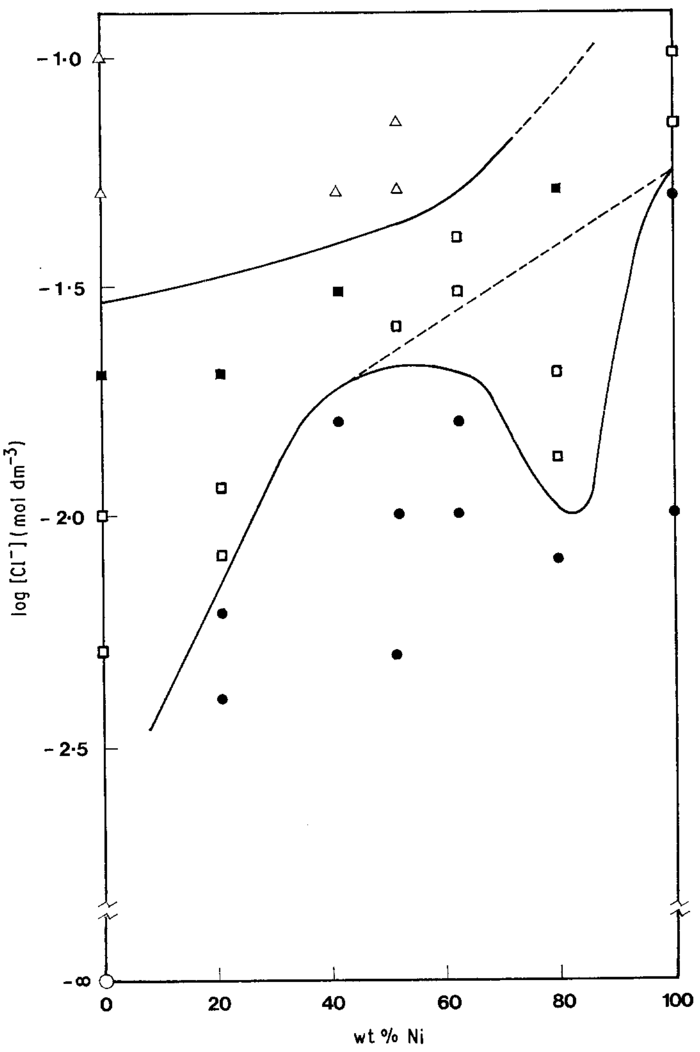

Figure 4 The passivation, pitting and general dissolution behaviour of Fe–Ni alloys anodically polarized in 0.5 M H_2SO_4 as a function of [Cl^-]. ●, passive; □, pitted; ■, pitted/dissolution; △, general dissolution.

NiO_{1+x} and a highly nonstoichiometric form written [Ni_2O_3] [15]. Such oxides are similar to those thermally formed on iron [26] and nickel [27], and in the absence of data on the anodically formed films on Fe–Ni alloys, we may consider the thermodynamics of the Fe–Ni–O system [28] and the oxides thermally formed on Fe–Ni alloys. The oxides FeO, Fe_3O_4, Fe_2O_3 thermally formed on pure iron are progressively replaced by Fe_3O_4, Fe_2O_3, $Ni_xFe_{3-x}O_4$ spinel, $Ni_{1-x}Fe_xO$ solid solutions, and $Ni_{1-x}O$, sometimes as duplex layers, as the nickel composition of the alloy is increased [27, 29–31]. On this basis it is possible that the austenitic alloys containing more than 80% Ni exhibit nickel-like behaviour (Fig. 3) because the passive film consists of NiO_{1-x} or $Ni_{1-x}Fe_xO$, and the austenitic alloys containing 40 to 60% Ni exhibit iron-like behaviour because the passive film consists of the iron-based spinel $Ni_xFe_{3-x}O_4$. On iron and iron-rich alloys the surface film is known to be based on Fe_3O_4/Fe_2O_3 [25]. The diffusion rate of iron in nickel ferrite spinel is much lower than in Fe_3O_4 [32], and also lower than the diffusion of cations in iron doped NiO [29]. Thus the low i_p values (when the concentration of Cl^- is zero) of alloys containing 40 to 60% Ni (Fig. 3) is consistent with the presence of a spinel type passivating surface layer.

According to Galvele [33] no pitting potential is found with iron, nickel and an Fe–25% Ni alloy in sulphuric acid solution as the Cl^- content of the solution is increased. Instead, over a range of potentials, pitting is induced as a process of chemical depassivation along with the continuous increase in the current density of the passive zone. This has been observed with all alloys in the Fe–Ni series (Figs 1 and 3). For pitting to occur a minimum concentration of Cl^- is required. This is 0.0003 M for pure iron [34]. Data for the Fe–Ni system from the present work are shown in Fig. 4. It is seen that the minimum concentration of Cl^- to cause pitting increases sharply as the composition of the alloy increases to about 25 to 30% Ni and then the change is more gradual up to 100% Ni. The value of 25 to 30% Ni occurs with the elimination of the ferrite phase in the alloys and hence the less corrosion resistant surface layer [20]. The dip in the curve at 80% Ni is considered anomalous and this point is discussed below.

Pitting morphologies were studied to only a limited extent and representative features are shown in Fig. 5. Morphologically there are two types of pits; etching pits with more or less crystallographically defined surface segments and brightening pits with more or less hemispherical form suggesting a degree of electrobrightening [35]. Pits in iron (Fig. 5a) were brightening pits and pits in nickel (Fig. 5g) were etching pits. Pits in the 40 and 60% Ni alloys (Figs 5c and d, respectively) tended towards an incomplete brightening pit hence showing iron-like behaviour. In the 20% Ni alloy the pits were brightening pits but were

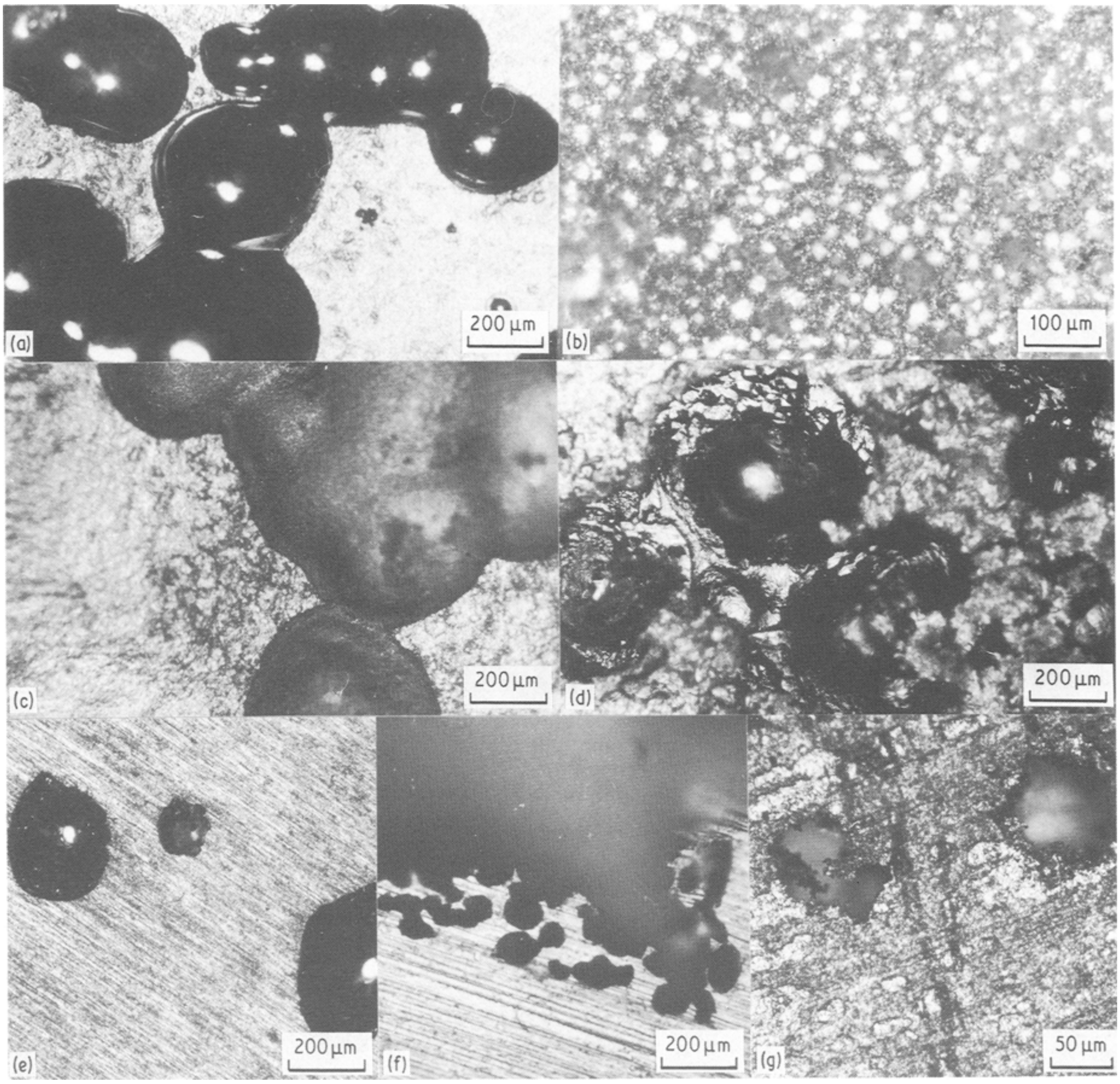

Figure 5 The characteristic features of pits formed on Fe–Ni alloys anodically polarized in 0.5 M H_2SO_4 containing Cl^-. (a) iron, (b) 20% Ni, (c) 40% Ni, (d) 60% Ni, (e) 80% Ni, (f) 80% Ni, (g) nickel. All are surface views except (f) which shows the cross-section of a tunnelling pit in the 80% Ni alloy.

unusually small and numerous (Fig. 5b) due, most probably, to the high inclusion content of the 20% Ni alloy. Of particular interest is the morphology of the pits in the 80% Ni alloy. Here it is seen that a certain amount of tunnelling has occurred as the pit grew into the metal (Fig. 5f). This is only observed with the 80% Ni alloy and we note that an order/disorder transformation of $FeNi_3$ occurs in the composition range from about 50 to 80 at % Ni centred on the composition 75 at % Ni [36]. Although there is no indication in the present work of superlattice $FeNi_3$ formation it is possible that some segregation towards the superlattice arrangement may have occurred. In this case selective dissolution of iron is possible along channels as suggested by Tammann in his theory of parting limits [37], or by Forty and co-workers [38, 39] who propose a corrosion pitting and tunnelling process involving selective dissolution and surface reordering. A more general viewpoint considers the selective dissolution of the more electronegative element with causes the collapse of the remaining lattice to form channels for solution intrusion [40]. Since a limited amount of tunnelling is observed (Fig. 5f), it may be that selective dissolution of iron is occurring by one of the above processes. This idea is supported by the data of Fig. 4 which shows the 80% Ni alloy to pit at low chloride concentrations characteristic of iron-rich alloys. In addition the dissolution of the 80% Ni alloy in solutions of a high Cl^- concentration adopts the very high i_p and i_{max} values again characteristic of the iron-rich alloys (Table II).

Overall, the main results of the present work are summarized and compared in Table III. Breaks in the corrosion properties occur between 20 and 40% Ni and between 60 and 80% Ni; say nominally at 30 and 70% Ni, respectively. The presence of ferrite determines the corrosion properties up to 30% Ni. The Fe–Ni system is thermodynamically not too far away from an ideal solid solution [41] and the thermodynamic activity in the austenite will decrease continuously with increase in nickel content of the alloy. Presumably, the break at 70% Ni is where the activity of the iron in the alloy falls below the activity of the nickel. That the change occurs in a relatively nickel-

TABLE III The alloy composition ranges of the corrosion properties of iron–nickel alloys anodically polarized in deoxygenated 0.5 M H_2SO_4 containing Cl^-; ⟶, ⟵, and - - - show the range of the iron-like property, nickel-like property, and possible range of the property, respectively

	Alloy composition (% Ni)					
	0	20	40	60	80	100
Crystal structure	bcc	bcc	fcc	fcc	fcc	fcc
E_{corr}	——	——→	←——	——	——	——
Active loop	——	——	——	——→	←——	——
i_p ($[Cl^-] = 0$)	——	——→	←——	——→	←——	——
i_p (slope)	——	——→	- - -	- - -→	←——	——
min Cl^- for pitting	——	——	← - - -	- - -	*← - - -	- - -
Pitting morphology	——	—— - - -	- - -	- - -→	*← - - -	- - -

*Indicates an anomalous result.

rich solid solution is consistent with the iron being more chemically active than the nickel.

4. Conclusions

From the present work on the anodic polarization of Fe–Ni alloys in de-oxygenated 0.5 M H_2SO_4 containing Cl^- we conclude:

1. Breaks occur in the value of the corrosion properties at 30 and 70% Ni.

2. The corrosion properties up to 30% Ni are determined by the presence of ferrite, and the low corrosion resistance of its surface film.

3. Iron-like behaviour extends to 70% Ni for some properties.

4. Austenitic alloys have a corrosion potential similar to the corrosion potential of nickel.

5. The change at 70% Ni is probably due to the thermodynamic activity of the iron in this and higher nickel alloys falling below that of the nickel.

6. Nickel-like behaviour occurs in alloys containing upwards of 70% Ni.

7. It is considered that a corrosion resistant nickel ferrite spinel type passivating layer exists on alloys containing 30 to 70% Ni.

8. Anomalous results occur with the 80% Ni alloy. These are considered to be due to the segregation tendency in the alloy to form the compound $FeNi_3$.

Acknowledgements

The authors wish to thank Inco Alloys International Ltd for the alloys containing 40 to 100% Ni, and Mr B. Hollyoak for the XRD and XRF analyses.

References

1. R. LANDAU and C. S. ODACH, *Trans. Electrochem. Soc.* **81** (1942) 521.
2. G. ECONOMY, R. SPEISER, F. H. BECK and M. G. FONTANA, *M. G. FONTANA, J. Electrochem. Soc.* **108** (1961) 337.
3. R. R. SAYANO and K. NOBE, *Corrosion* **22** (1966) 81.
4. F. ZUCCHI, G. GILLI, P. A. BOREA and G. TRABANELLI, *Corros. Sci.* **12** (1972) 669.
5. K. SHIOBARA, Y. SAWADA and S. MORIOKA, *Trans. Jpn Inst. Metals* **6** (1965) 97.
6. D. O. CONDIT, *Corros. Sci.* **12** (1972) 451.
7. H. H. UHLIG, *Z. Electrochem.* **62** (1958) 700.
8. F. WENCAP and J. CALLAND, in "Passivity of Metals and Semiconductors", edited by M. Froment (Elsevier, Amsterdam, 1984) p. 649.
9. D. O. CONDIT, in Proceedings of the 5th Interantional Congress on Metallic Corrosion, Tokyo 1972 (National Association of Corrosion Engineers, Houston, 1974) p. 16.
10. *Idem, Corrosion* **28** (1972) 93.
11. C. FIAUD and A. KADRI, *Mater. Chem. Phys.* **9** (1983) 529.
12. A. BENGALI and K. NOBE, *J. Electrochem. Soc.* **126** (1979) 1118.
13. B. MacDOUGAL and M. COHEN, *ibid.* **124** (1977) 1185.
14. K. ASAMI and K. HASHIMOTO, *Corros. Sci.* **24** (1984) 83.
15. S. G. REAL, J. R. VILCHE and A. J. ARVIA, *ibid.* **20** (1980) 563.
16. V. HOSPADARUK and J. V. PETROCELLI, *J. Electrochem. Soc.* **113** (1966) 787.
17. R. C. V. PIATTI, A. J. ARVIA and J. J. POEDSTRA, *Electrochim. Acta* **14** (1969) 541.
18. G. M. SCHMID and N. HACKERMAN, *J. Electrochem. Soc.* **108** (1961) 741.
19. K. NOBE and R. F. TOBIAS, *Corrosion* **20** (1964) 263t.
20. K. SUGIMOTO and S. MATSUDA, *J. Electrochem. Soc.* **130** (1983) 2323.
21. N. SATO and G. OKAMOTO, in "Comprehensive Treatise on Electrochemistry" Vol. 4, edited by J. O'M. Bockris, B. E. Conway, E. Yeager and R. E. White (Plenum, New York 1981) p. 193.
22. J. L. DELPLANCKE, *Surface Tech.* **20** (1983) 71.
23. T. E. POU, O. J. MURPHY, V. YOUNG, J. O'M. BOCKRIS and L. L. TONGSON, *J. Electrochem. Soc.* **131** (1984) 1243.
24. C. L. FOLEY, J. KRUGER and C. J. BECHTOLDT, *ibid.* **114** (1967) 894.
25. J. M. WEST, in "Basic Corrosion and Oxidation" (Ellis-Horwood, Chichester, 1980) p. 109.
26. I. A. MENZIES and W. J. TOMLINSON, *J. Iron Streel I* **204** (1966) 1239.
27. W. J. TOMLINSON, *J. C. S. Faraday I* **73** (1977) 1334.
28. A. D. DALVI and W. W. SMELTZER, *J. Electrochem. Soc.* **117** (1970) 1431.
29. *Idem, ibid.* **118** (1971) 1978.
30. W. J. TOMLINSON, M. J. GARDNER and R. J. KOWALSKI, *Corros. Sci.* **17** (1977) 301.
31. G. L. WULF, T. J. CARTER and G. R. WALLWORK, *ibid.* **9** (1969) 689.
32. R. H. CONDIT, M. J. BRABERS, and C. E. BRICHENALL, *Trans. Met. Soc. AIME* **218** (1960) 768.
33. J. R. GALVELE, in "Passivity of Metals", edited by R. P. Frankenthal and J. Kruger, (The Electrochemical Society, New Jersey, 1978) p. 285.
34. N. D. STOLICA, *Corros. Sci.* **9** (1969) 455.
35. N. SATO, *J. Electrochem. Soc.* **129** (1982) 260.
36. R. J. WAKELIN and E. L. YATES, *Proc. Phys. Soc.* **B66** (1953) 221.
37. G. TAMMANN, *Z. Anorg. Chem.* **107** (1919) 1.
38. A. J. FORTY and P. DURKIN, *Phil. Mag.* **42** (1980) 295.
39. A. J. FORTY and G. ROWLANDS, *ibid.* **43** (1981) 171.
40. M. J. PRYOR and J. C. FISTER, *J. Electrochem. Soc.* **131** (1984) 1230.
41. R. A. ORIANI, *Acta Metall.* **1** (1953) 448.

Received 31 May 1985
and accepted 7 January 1986